CGMS-XXVIII JPN-WP-11
Prepared by JAPAN
Agenda Item:II/2

PRELIMINARY STUDY ON INTER-CALIBRATION OF THE VISIBLE CHANNEL BETWEEN GMS-5 AND NOAA-14

The purpose of this paper is to present the results of preliminary study on inter-calibration of the visible channels between GMS-5 and NOAA-14 in the case of clear and cloudy conditions.

Preliminary Study on Inter-calibration of the Visible Channel between GMS-5 and NOAA-14

1. INTRODUCTION

MSC/JMA carried out the study on inter-calibration of the infrared channels between GMS-5 VISSR and NOAA-14 AVHRR in 1998. The Results showed that the GMS-5 VISSR temperature was statistically about 1.2 K colder than the NOAA-14 AVHRR temperature. In the 27th CGMS meeting, MSC presented that the square of value of GMS-5 visible level was linearly related to the value of NOAA-14 AVHRR visible level with approximately 0.76 of correlation coefficient in the case of clear condition. MSC continues further inter-calibration activities to other region (e.g. desert, cloud). This report shows the preliminary results in the case of including both clear and cloudy conditions.

2. DATA SELECTION AND METHOD

The target regions are selected when the following conditions are satisfied.

- The target region is enclosed by 15N-15S and 125E-155E latitude / longitude lines near sub-satellite point of GMS-5.
- The difference of observational time between GMS-5 and NOAA-14 is within 15 minutes to reduce variability of cloudy conditions.
- The region contains clear areas and cloudy areas to make a uniform distribution statistically.

The selected region is subdivided into grid areas (0.25 latitude x 0.25 longitude) and the sub-grid areas are further selected when the following conditions are satisfied.

The view angles of the sub-grid areas are within 50 degrees from the nadir of NOAA-14 to minimize undesirable effects, i.e., the difference in the atmospheric effect due to the difference of observational path and the difference in the spatial resolution between the nadir and the limb of observation.

The sun-glint angles of sub-grid areas are over 10 degrees to both satellites to reduce the sun-glint effect.

The sub-grid areas have samples over 10 pixels to keep enough samples statistically.

The mean and variance of albedo in every selected sub-grid areas are computed for both GMS-5 and NOAA-14 by taking the average of albedo to 90 % level from its minimum of cumulative frequency of the histogram. The sub-grid areas are finally selected in the condition of the variance of NOAA albedo is within 5 levels and that of GMS is within one level when the mean of albedo is less than 10 % corresponding to clear area. The other sub-grid areas are also selected in the condition of the variance of NOAA albedo is within 15 levels and that of VISSR is within 2 levels when the mean of albedo is larger than 10 % corresponding to cloudy area. The mean of albedo is corrected by multiplying the term 1 / cos (sun zenith angle), and then the average albedo of all the selected sub-grid areas for each satellite is compared.

The first straight line related the average value of GMS and NOAA albedo is determined by the method of least squares, and then data with over 12 % deviation from the straight line to clear area and with over 24 % deviation from the line to cloudy area are rejected. The second straight line is determined once again by the same method using the remaining data, and then data with over 6 % deviation from the straight line to clear area and with over 12 % deviation from the line to cloudy area are rejected. In the same method, data with over 3 % deviation to clear area and with over 6 % deviation are rejected again, and the final straight line is determined using the remaining data.

3. RESULTS

The four cases are investigated, and their results are shown in Table-1. The results show that discrepancies of among each straight line determined in different observations appears. To minimize the discrepancy, a straight line is determined again using all data shown in Table-1.

Fig. 1 shows a scatter diagram for all data between GMS-5 and NOAA-14 before the procedure for rejecting inappropriate data. Fig. 2 shows a scatter diagram for all data adopted finally. The remaining data finally are declined to seven-eighth of all data after the procedure of rejection. The remaining sub-grids finally are also about 3 % of all sub-grids used for the study. Thus it appears that the number of appropriate sub-grids for the study is very small.

The final fitting equation is NOAA albedo = 0.8106 * GMS albedo + 4.9126 (%) and the equation is determined with a high correlation coefficient, 0.99. A dashed line in Fig. 2 is the result of inter-calibration in March 2000 performed in the ISCCP calibration center in France. The equation is shown as NOAA albedo = 0.8640 * GMS albedo + 1.98 (%). The discrepancy is several percent between the values of NOAA albedo converted from GMS albedo using our equation and the corresponding values given by the ISCCP equation. It is inferred that the intercept term of our equation is larger than that of ISCCP since GMS albedo is extremely small in clear areas.

Table-1

Straight lines related between NOAA albedo (y-axis) and GMS albedo (x-axis). NOAA Time and GMS Time: Observational time on the equator (UTC). Time Dif.: observational time difference between both satellites (minute). Num.: Number

Date	NOAA Time	GMS Time	Time Dif.	Target Region	Equation	Num.
Jan.20, 2000	**05:59**	**05:45**	**14**	**(10N,135E)-(5S,155E)**	**y = 0.8208x + 3.819**	**563**
Mar.26, 2000	**06:47**	**06:45**	**2**	**(15N,125E)-(5S,155E)**	**y = 0.7941x + 4.774**	**484**
May 09, 2000	**06:44**	**06:45**	**1**	**(15N,125E)-(5S,155E)**	**y = 0.7747x + 7.4801**	**525**
May 26, 2000	**06:48**	**06:45**	**3**	**(15N,125E)-(5S,155E)**	**y = 0.8516x + 4.8921**	**772**

4. CONCLUSION

The present result is the same as that of inter-calibration of ISCCP on the whole although the fitting equations largely vary by each observations. We have a possibility that this method leads to monitoring of calibration of NOAA and GMS routinely through further evolution of the technique and the increase of sampling data.

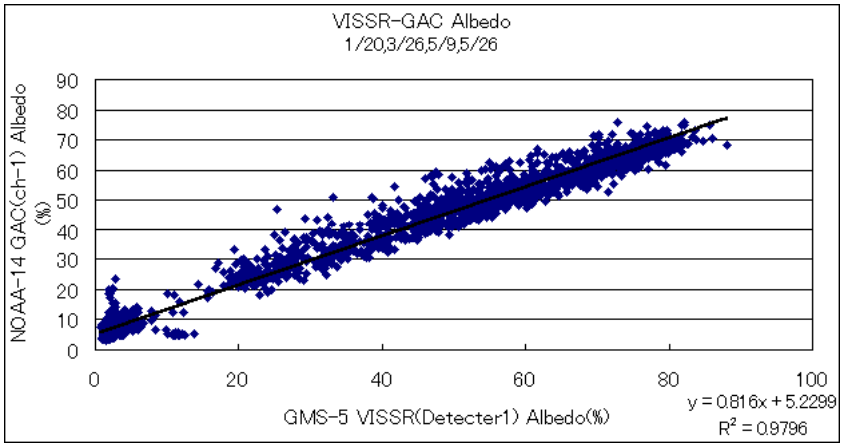

Fig. 1 A scatter diagram before the procedure of rejection.

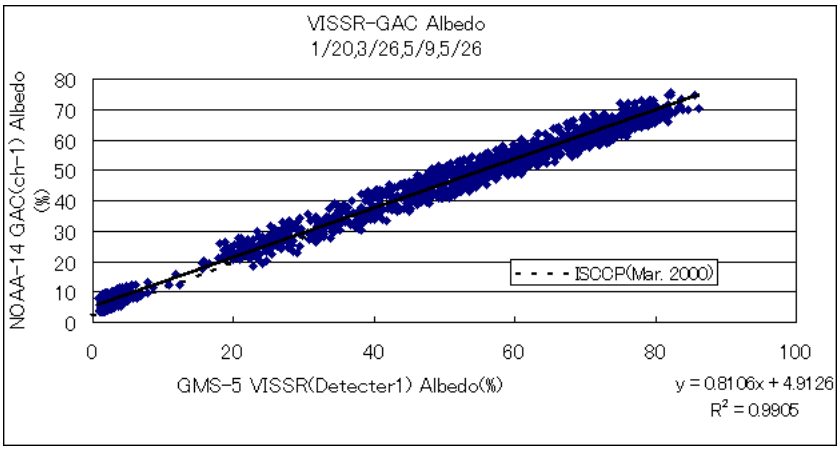

Fig. 2 A scatter diagram after the procedure of rejection.